Zimbabwe Agroclimatic Similarity

Alex Ruane[1], Sanketa Kadam[1,2], Sabine Homann Kee-Tui[3], Carolyn Mutter[1,2] and Kathryn Longobardi[1]

[1] NASA Goddard Institute for Space Studies, New York, USA

[2] Columbia University Center for Climate Systems Research, New York, USA

[3] International Crops Research Institute for the Semi-Arid Tropics, Bulawayo, Zimbabwe

December 1st, 2021

Motivation

Earlier AgMIP integrated assessments focused on sub-national regions (on the scale of a district or network of neighboring villages) in order to characterize farming systems, climate hazards, agricultural vulnerabilities and opportunities for adaptation (Rosenzweig et al., 2015; 2021). These regions were selected according to their prominence as agricultural production areas, representative farming systems, engagement with local stakeholders and the availability of climate, crop, livestock and economic data. Results in these sub-national regions proved useful in assessing climate risk and the potential for a number of adaptation options; however, uncertainty concerning the extent to which these results could be transferred to other regions/systems or scaled up to national scales limited the overall utility of these findings for broader climate resilience planning. This project therefore explored a number of approaches to relate local and national scale conditions in order to understand where findings and key messages would likely be transferable.

Approach

Similarity between regional systems can be characterized by a combination of climatic conditions, biophysical conditions on the farm, and socioeconomics. Further distinction could be determined by similarity today (i.e., under present climate and farm systems) and similarity in the future (i.e., under future climate and farm systems). Here we demonstrate agroclimatic similarity analyses over the Zimbabwe component of the AgMIP/CLARE project, focusing on the Nkayi district and household survey that was the focus of previous analyses and connecting into ongoing efforts within the country to update agro-ecological zones (AEZ) for the first time since the 1960s. Similar analyses were initiated in Ghana and Senegal as a proof of transferable approaches, but these are not the focus of discussion here.

The core approach develops a portfolio of observational and modeled layers that characterize one aspect of farm conditions across Zimbabwe (climate, crop, livestock, and economics; today and in future), determines conditions in Nkayi for that layer, establishes a range of conditions considered "similar" to the Nkayi condition for each layer, then identifies other regions in Zimbabwe that are within this range and therefore similar to Nkayi and likely to face similar challenges and opportunities to the farm households studied there. Details of the specific biophysical, current climate (focusing on the maize-growing season), future climate (under a high emissions [RCP8.5] scenario for mid-century [2040-2070] conditions), climate change (future compared to present), and socioeconomic layers are provided in **Table 1** which details each variable layer name, unit, spatial resolution, temporal resolution, time period, Nkayi value, Nkayi "similarity" range, and data description. Layers include biophysical information from satellite vegetation indices (such as the Enhanced Vegetation Index; EVI), land variables

(including soil moisture and established agro-ecological zones, AEZ, updated in 2020 by the Zimbabwe National Geospatial and Space Agency), climate variables including average growing season conditions (e.g., temperature, precipitation), the frequency of extreme climate events (e.g., days where temperatures exceed 35°C), and socioeconomic conditions (e.g., livelihood zones and cattle density). As climate challenges reflect both difficult conditions as well as the rate of change that forces responses, climate conditions are given for current climate, future climate, and the amount of climate change.

Table 1: Layers factored into agroclimatic similarity analysis for Nkayi, Zimbabwe.

	Variable Layer Name	Units	Product Spatial Resolution	Product Temporal Resolution	Evaluation Period	Nkayi farms avg value	Similarity Range	Product Description
Biophysical Layers	**Mean NDVI***	NA	250 m	16-Day	2000-2020	--	--	MOD13Q1 MODIS/Terra Vegetation Indices 16-Day L3 Global 250m SIN Grid V061 (Didan, 2021)
	Min NDVI*	NA	250 m	16-Day	2019- 2020	--	--	MOD13Q1 MODIS/Terra Vegetation Indices 16-Day L3 Global 250m SIN Grid V061 (Didan, 2021)
	Max NDVI*	NA	250 m	16-Day	2019- 2020	--	--	MOD13Q1 MODIS/Terra Vegetation Indices 16-Day L3 Global 250m SIN Grid V061 (Didan, 2021)
	Mean EVI	NA	1km	16-Day	2000-2020	0.2661	0.2394 to 0.2927	MOD13A2 MODIS/Terra Vegetation Indices 16 Day L3 Global 1km SIN Grid V61 (Didan, 2021)
	Min EVI	NA	1km	16-Day	2000-2020	0.0935	0.0692 to 0.0622	MOD13A2 MODIS/Terra Vegetation Indices 16 Day L3 Global 1km SIN Grid V61 (Didan, 2021)
	Max EVI	NA	1km	16-Day	2000-2020	0.6252	0.5462 to 0.6008	MOD13A2 MODIS/Terra Vegetation Indices 16 Day L3 Global 1km SIN Grid V61 (Didan, 2021)
	DOY min EVI*	Julian Day	1km	16-Day	2000-2020	--		MOD13A2 MODIS/Terra Vegetation Indices 16 Day L3 Global 1km SIN Grid V61 (Didan, 2021)
	DOY max EVI*	Julian Day	1km	16-Day	2000-2020	70	65-75	MOD13A2 MODIS/Terra Vegetation Indices 16 Day L3 Global 1km SIN Grid V61 (Didan, 2021)
Land Layers	**Land Cover***	Classes	1km	10-year	2010-2019	--	--	MCD12Q2 Land Cover Dynamics Yearly L3 Global 1km (Friedl et al, 2019)
	Soil Moisture Profile	Root-zone fraction	10 Km	3-Day composites	2016-2020	0.25	0.225 to 0.275	NASA- USDA Enhanced SMAP Global Soil Moisture Data (Mladenova et al 2020)
	Subsurface Soil Moisture	mm	10 Km	3-Day composites	2016-2020	25.87	23.283 to 28.457	NASA- USDA Enhanced SMAP Global Soil Moisture Data (Mladenova et al 2020)
	Agro-Ecological Zone (AEZ)	NA	NA	1-year	2020	III & IV	III & IV	Zimbabwe National Geospatial and Space Agency
Current Climate Layers **	**# Extreme Heat Days (Tmax > 35 °C)**	Days	0.5˚	Daily	1990-2020	5	4 to 6	ISIMIP3 Ensemble of 5 Bias-adjusted General Circulation Models (GCMs; Lange et al., 2019)
	Total Precipitation	mm	0.5˚	Daily	1990-2020	636	572 to 700	ISIMIP3 Ensemble of 5 Bias-adjusted General Circulation Models (GCMs; Lange et al., 2019)
	Mean Temperature	°C	0.5˚	Daily	1990-2020	23.2	20 to 25	ISIMIP3 Ensemble of 5 Bias-adjusted General Circulation Models (GCMs; Lange et al., 2019)
	# Rainy Days (P > 1 mm)	Days	0.5˚	Daily	1990-2020	59	52 to 65	ISIMIP3 Ensemble of 5 Bias-adjusted General Circulation Models (GCMs; Lange et al., 2019)
Future Climate Layers **	**# Extreme Heat Days (Tmax > 35 °C)**	Days	0.5˚	Daily	2040-2070 (SSP585)	30.5714	27 to 34	ISIMIP3 Ensemble of 5 Bias-adjusted General Circulation Models (GCMs; Lange et al., 2019)
	Total Precipitation	mm	0.5˚	Daily	2040-2070 (SSP585)	672.8741	605 to 740	ISIMIP3 Ensemble of 5 Bias-adjusted General Circulation Models (GCMs; Lange et al., 2019)
	Mean Temperature	°C	0.5˚	Daily	2040-2070 (SSP585)	25.57	23 to 28	ISIMIP3 Ensemble of 5 Bias-adjusted General Circulation Models (GCMs; Lange et al., 2019)
	# Rainy Days (P > 1 mm)	Days	0.5˚	Daily	2040-2070 (SSP585)	57.92	52 to 64	ISIMIP3 Ensemble of 5 Bias-adjusted General Circulation Models (GCMs; Lange et al., 2019)
Future Climate Change Layers **	**Change in # Extreme Heat Days (Tmax > 35 °C)**	Days	0.5˚	30-year means	SSP585 2040-2070 vs. 1990-2020	25.5	23 to 28	ISIMIP3 Ensemble of 5 Bias-adjusted General Circulation Models (GCMs; Lange et al., 2019)
	Change in Total Precipitation	% of baseline	0.5˚	30-year means	SSP585 2040-2070 vs. 1990-2020	-0.6783	-0.61 to -0.75	ISIMIP3 Ensemble of 5 Bias-adjusted General Circulation Models (GCMs; Lange et al., 2019)
	Change in Mean Temperature	°C	0.5˚	30-year means	SSP585 2040-2070 vs. 1990-2020	2.38	2.28 to 2.45	ISIMIP3 Ensemble of 5 Bias-adjusted General Circulation Models (GCMs; Lange et al., 2019)

	Change in # Rainy Days (P > 1 mm)	Days	0.5˚	30-year means	SSP585 2040-2070 vs. 1990-2020	-1.215	-1.0 to -1.33	ISIMIP3 Ensemble of 5 Bias-adjusted General Circulation Models (GCMs; Lange et al., 2019)
Socioeconomic Layers	**Population Density**	persons / km	1 Km	5-year	2000	20.98	18 to 22	Gridded Population of the World, Version 4 (GPWv4.11): Population Density Adjusted to Match 2015 Revision of UN WPP Country Totals (CIESIN - Columbia University. 2018.)
	Population Density	persons / km	1 Km	5-year	2020	26.146	23.5 to 28.75	Gridded Population of the World, Version 4 (GPWv4.11): Population Density Adjusted to Match 2015 Revision of UN WPP Country Totals (CIESIN - Columbia University. 2018.)
	Livestock Density- Cattle	# cattle / pixel	0.83˚	1-year	2010	1527.128	1374 to 1680	Gridded Livestock of the World database (GLW 3)- Global Cattle Distribution (Gilbert et al, 2018)
	Livelihoods*	NA	NA	1-year	2020	ZW09	ZW09, 16, 17, 21, 24	Zimbabwe National Geospatial and Space Agency (ZINGSA), 2020

* Layer not a focus of current analyses
** Calculated over the Maize growing season for each ½ degree pixel (Müller et al., 2017)

Similarity ranges for quantitative variables were determined by first calculating the average of the values for the 7 villages included in the Nkayi farm survey. A first guess of ±10% set the range of similarity, with each layer further examined to ensure that this range of similarity helped distinguish conditions across Zimbabwe (that is, a layer where the whole country is considered "similar" does not add distinguishing regional information). Combinations of layers were then used to provide similarity "scores" for each part of Zimbabwe that reflect the number of layers within a given set that are similar to Nkayi. These scores are not weighted toward any individual layers other than in the selection of the inclusive set, so the analysis below forms a starting point for deeper analysis depending on the specific interventions that may target hazard resilience in vulnerable communities.

Key findings

No single combination of layers is sufficient to capture the many differences in Zimbabwe's diverse landscape, so we examine a variety of layer combinations to provide multiple perspectives on the common challenges and unique characteristics of agroclimatic conditions.

1. Current biophysical similarity

Figure 1 highlights areas within Zimbabwe that have a similar seasonal progression of vegetation to that observed in Nkayi. The average EVI describes the overall level of vegetation, which is a proxy for overall productivity and potential fodder for livestock. Maximum and minimum EVI values describe the annual amount of vegetation growth and dieback that highlights the best conditions and the lean months, while the day of the year for maximum EVI pins the vegetation growth to major seasonal patterns of temperature and rainfall that could distinguish different regional climates. Put together as a similarity score, there is no clear regional pattern of EVI characteristics that distinguish different portions of Zimbabwe, indicating that the overall vegetation pattern is quite similar across the country. Within each region there is strong heterogeneity, however, indicating sharp patterns in land management and contrasts between agricultural lands and unmanaged lands that could be natural or utilized for grazing.

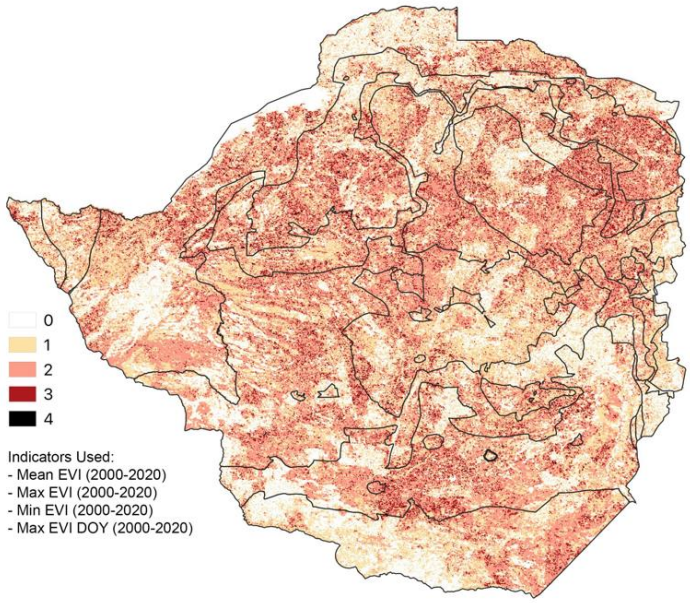

Figure 1: *Current biophysical similarity score calculated from 4 similarity layers drawn from the 2000-2020 period: mean EVI, annual maximum EVI, annual minimum EVI, and the day of the year on which maximum EVI is observed.*

2. Current climate similarity

The mean and extreme characteristics of Nkayi climate is similar to a broad swath across the center of Zimbabwe, as well as portions of the Northeast (**Figure 3.5.2**). The southernmost portions of the country share few characteristics with Nkayi climate.

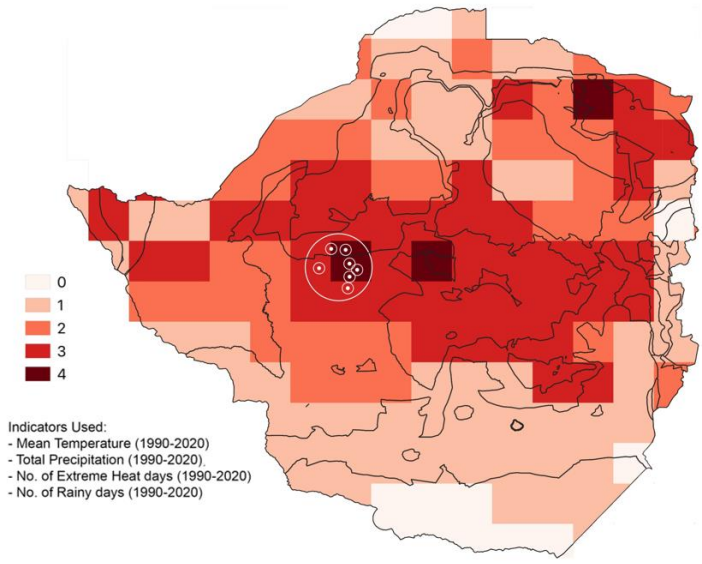

Figure 2: *Current climate similarity score calculated from 4 similarity layers drawn from the 1990-2020 period: mean temperature, total precipitation, the number of extreme heat days (Tmax > 35℃), and the number of rainy days (P>1mm). The locations of the 7 surveyed Nkayi villages are shown as white circles within the broader Nkayi region.*

3. Current agroclimatic similarity

The combination of core climate variables, soil moisture, and vegetation seasonal cycle reveals a slight Northwest to Southeast swath of the country that is similar to Nkayi (**Figure 3.5.3**). In contrast to the climate-only similarity that was oriented in a more West-East pattern, interactions with soil conditions and vegetation show that regions along this more diagonal axis are likely to have similar conditions for agriculture. Comparisons against the livelihoods zone layer (ZINGSA, 2020) indicate that many of the zones that are highly similar to Nkayi on this combination of layers are also areas with prominent smallholder agriculture and mixed cereal-livestock systems. These zones are most likely to face challenges to agricultural adaptation and resilience planning that were extensively explored at Nkayi. Note that the resolution of the EVI seasonality layer is finer than the other layers, with many pixels similar across all 4 layers even as the other layers set the broader patterns.

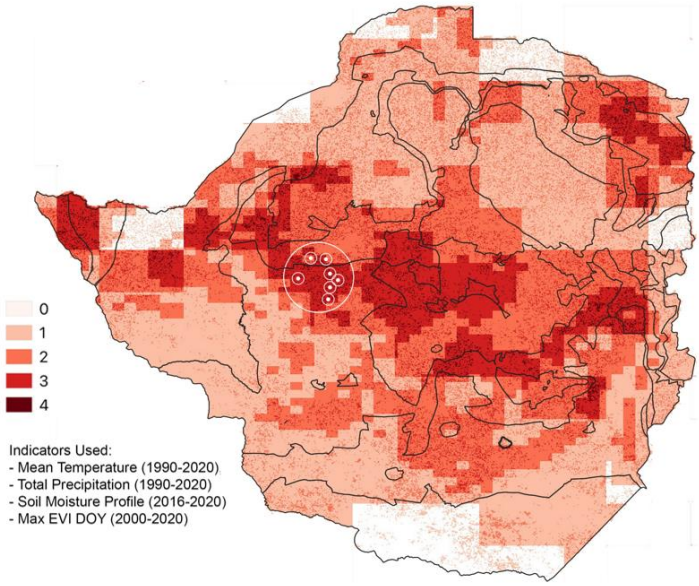

Figure 3: *Current agroclimatic similarity score calculated from 4 similarity layers drawn from recent observations: mean temperature, total precipitation, soil moisture profile saturation, and day of year for maximum EVI. The locations of the 7 surveyed Nkayi villages are shown as white circles within the broader Nkayi region.*

4. Climate change rate similarity

The rate of climate change experienced provides another perspective on adaptation and resilience planning similarity across regions within Zimbabwe (**Figure 3.5.4**). Climate change in Nkayi is projected to be similar that for a North to South swath of Zimbabwe across the slightly more Western portion of the country. These regions may not have the same future conditions but are facing a similar degree of disruption in terms of climate changes. The pattern of changes for lower emissions scenarios (RCP4.5) examined in this study are similar even as the extent of climate change is reduced.

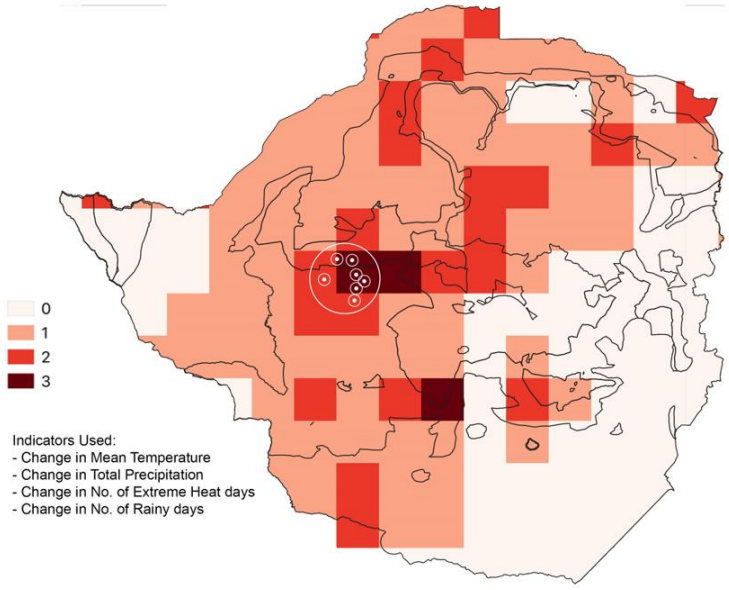

Figure 4: *Climate change rate similarity score calculated from 4 similarity layers calculated as the difference between future (RCP8.5 2040-2070) and current (1990-2020) periods: change in mean temperature, change in total precipitation, change in the number of extreme heat days (Tmax > 35℃), and change in the number of rainy days (P>1mm). The locations of the 7 surveyed Nkayi villages are shown as white circles within the broader Nkayi region.*

5. Future climate similarity

In the RCP8.5 mid-century (2040-2070) period Nkayi will continue to have a climate similar to the central part of the country, although it will be increasingly similar to the Northwestern portions of the Zimbabwe (**Figure 3.5.5**). In this sense adaptation and resilience planning actions between these regions will likely converge to reflect common conditions and climate challenges for agriculture.

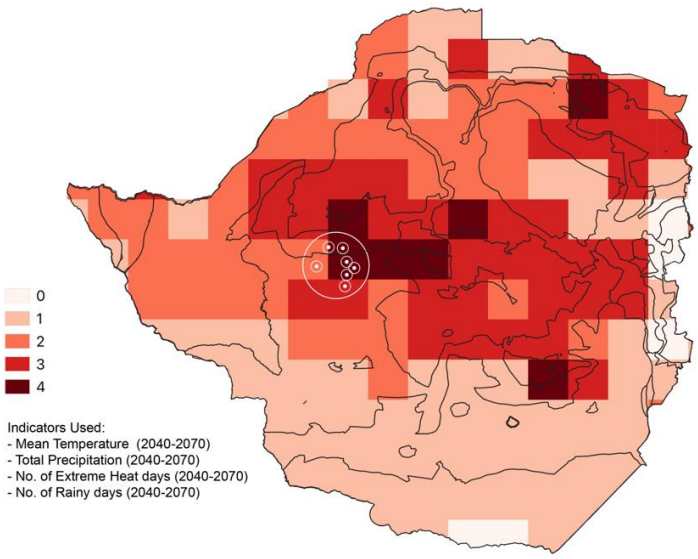

Figure 5: *Future climate similarity score calculated from 4 similarity layers drawn from the RCP8.5 2040-2070 period: mean temperature, total precipitation, the number of extreme heat days (Tmax > 35℃), and the number of rainy days (P>1mm). The locations of the 7 surveyed Nkayi villages are shown as white circles within the broader Nkayi region.*

6. Current climates that are similar to projected Nkayi climate

A comparison between Nkayi's future climate and the present climate of Zimbabwe shows that future conditions in Nkayi will be similar to conditions currently experienced in the northern portions of Zimbabwe, particularly those areas in the Northwest and Northeast (**Figure 3.5.6**). Adaptation and resilience planners in Nkayi might therefore look to present systems and climate risk planning in these portions of the country to anticipate solutions for their future challenges.

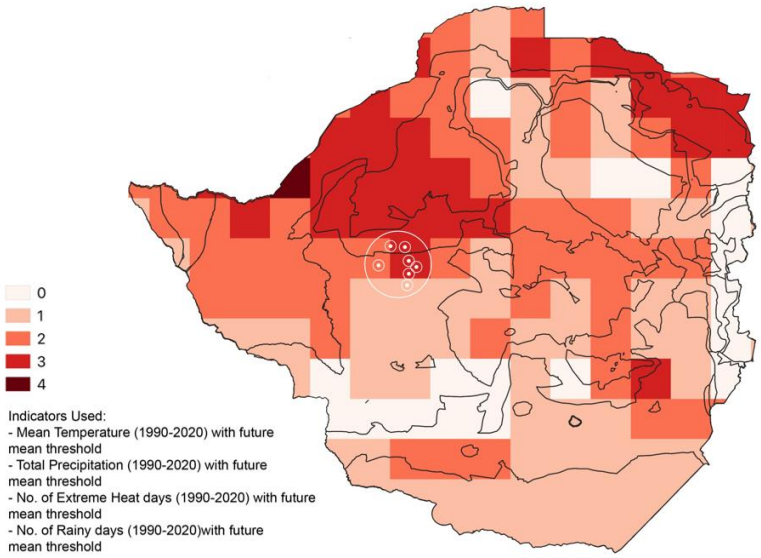

Figure 6: *Current climates that are similar to Nkayi's future climate; thresholds drawn from Nkayi's future climate projection and applied to current climate layers. Similarity score calculated from 4 similarity layers drawn from the 1990-2020 period: mean temperature, total precipitation, the number of extreme heat days (Tmax > 35C), and the number of rainy days (P>0.1mm). The locations of the 7 surveyed Nkayi villages are shown as white circles within the broader Nkayi region.*

7. Broad agro-climatic similarity

Figure 3.5.7 utilizes a broad set of biophysical, land, current climate and socioeconomic layers to identify regions that have strong acro-climatic similarity to Nkayi. The use of this many layers is instructive, but further analysis is needed to examine the specific combinations of similar layers for any given pixel. Overall similarity is strongest in the regions closest to the Nkayi farms and generally is reduced with distance, however higher similarity scores extend East into the center of the country and are also seen in the Northeast (between Mutoko and Mount Darwin) and far Western portions of Zimbabwe (southwest of Victoria Falls). Southernmost regions (near Beitbridge) and the Eastern area around Nyanga National Park are least similar, and therefore are not likely to be suitable for the adaptation and resilience planning efforts developed for Nkayi.

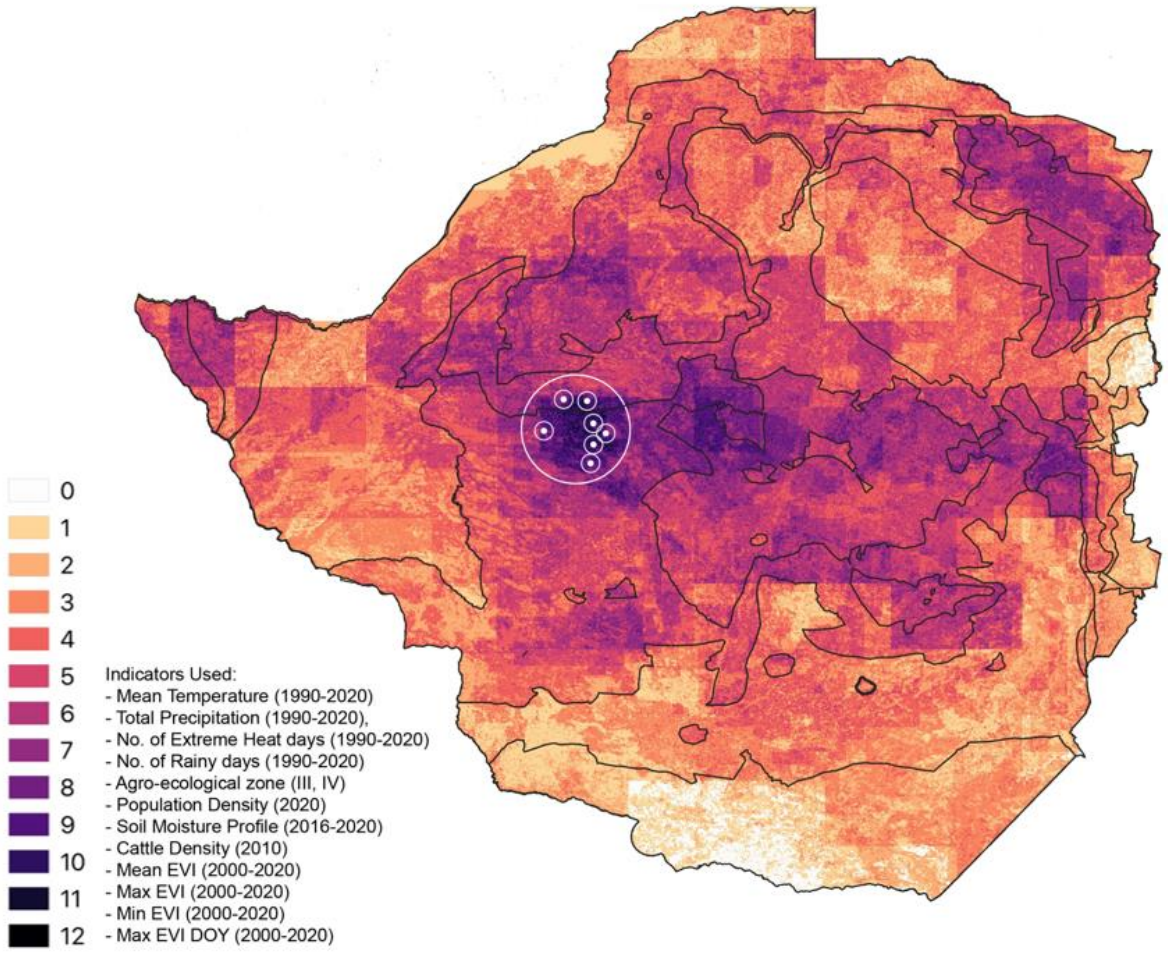

Figure 7: *Broad agro-climatic similarity score calculated from 12 similarity layers drawn from recent observational periods: mean temperature, total precipitation, the number of extreme heat days (Tmax > 35℃), the number of rainy days (P>1mm), Agro-ecological zone, population density, soil moisture profile saturation, cattle density, mean EVI, annual maximum EVI, annual minimum EVI, and day of year for the maximum EVI. The locations of the 7 surveyed Nkayi villages are shown as white circles within the broader Nkayi region.*

Opportunities for further application

Agroclimatic similarity analysis for Zimbabwe shows that adaptation and resilience challenges fall along geographical patterns that may be useful in efficiently transferring successful approaches from Nkayi to the broader country. In many cases Nkayi results are broadly applicable, but analysis indicates that there are not clear and coherent regions with identical conditions given the heterogeneity of climate and agricultural conditions within Zimbabwe. Other portions of Zimbabwe (or other countries) may be more broadly representative than Nkayi, and this type of analysis may identify wide areas where adaptation and resilience planning may be useful in less heterogeneous countries. Preliminary explorations of this approach in Ghana, for example, show strong zonal bands associated with the Savanah, Sahel, and tropical forest portions of the country, while Senegal analyses indicate strong coastal and inland patterns.

The current approach can also be improved by better connecting the range of "similar" conditions to specific agricultural vulnerability and adaptation and resilience plan tolerances.

For example, in the above analyses areas were considered similar to Nkayi if their total maize growing season precipitation was within 10% of the Nkayi value; however, additional information about farm system tolerances could more accurately set the range of plausible values for a given adaptation option and thus be more useful for planning. Continued engagement with local experts would also help identify additional layers and similarity thresholds that reflect the decision processes of stakeholders within the region (e.g., which seeds to plant, where to invest in livestock, whether irrigation is practical). Specific policies could also be targeted to a designed set of conditions that could be explored through geospatial analysis of these layers, either through a combined score based on custom ranges or on a multi-layer set of criteria to identify minimal conditions indicative of success.

Agroclimatic similarity analysis could also be combined with gridded crop modeling efforts (such as those piloted in Ghana) and national economic modeling (such as that piloted in Senegal) to build more efficient modeling systems that prioritize diverse systems or those with the highest economic impact or population vulnerabilities. Improved information about specific policies, adaptation investments, farm system transformations, and crop system responses to climate changes may also be factored into future analyses to inform more useful planning efforts.

References:

Bolten, J., W.T. Crow, X. Zhan, T.J. Jackson, and C.A. Reynolds (2010). Evaluating the Utility of Remotely Sensed Soil Moisture Retrievals for Operational Agricultural Drought Monitoring, IEEE Transactions on Geoscience and Remote Sensing, 3(1): 57-66. doi:10.1109/JSTARS.2009.2037163 Article Google Scholar

Bolten, J., and W. T. Crow (2012). Improved prediction of quasi-global vegetation conditions using remotely sensed surface soil moisture, Geophysical Research Letters, 39: (L19406). [doi:10.1029/2012GL053470][https://doi.org/10.1029/2012GL053470] Article Google Scholar

Center for International Earth Science Information Network - CIESIN - Columbia University. 2018. Gridded Population of the World, Version 4 (GPWv4.11): Population Density Adjusted to Match 2015 Revision of UN WPP Country Totals, Revision 11. Palisades, NY: NASA Socioeconomic Data and Applications Center (SEDAC). https://doi.org/10.7927/H4F47M65

Didan, K. (2021). MODIS/Terra Vegetation Indices 16-Day L3 Global 1km SIN Grid V061 [Data set]. NASA EOSDIS Land Processes DAAC. Accessed 2021-10-14 from https://doi.org/10.5067/MODIS/MOD13A2.061

Entekhabi, D, Njoku, EG, O'Neill, PE, Kellogg, KH, Crow, WT, Edelstein, WN, Entin, JK, Goodman, SD, Jackson, TJ, Johnson, J, Kimball, J, Piepmeier, JR, Koster, RD, Martin, N, McDonald, KC, Moghaddam, M, Moran, S, Reichle, R, Shi, JC, Spencer, MW, Thurman, SW, Tsang, L & Van Zyl, J (2010). The soil moisture active passive (SMAP) mission, Proceedings of the IEEE, 98(5): 704-716. doi:10.1109/JPROC.2010.2043918 Article

Friedl, M., Gray, J., Sulla-Menashe, D. (2019). MCD12Q2 MODIS/Terra+Aqua Land Cover Dynamics Yearly L3 Global 500m SIN Grid V006 [Data set]. NASA EOSDIS Land Processes DAAC. Accessed 2021-10-14 from https://doi.org/10.5067/MODIS/MCD12Q2.006

Gilbert, Marius; Nicolas, Gaëlle; Cinardi, Giusepina; Van Boeckel, Thomas P.; Vanwambeke, Sophie; Wint, William G. R.; Robinson, Timothy P., 2018, "Global cattle distribution in 2010 (5 minutes of arc)", https://doi.org/10.7910/DVN/GIVQ75, Harvard Dataverse, V3

Mladenova, I. E., J.D. Bolten, W.T. Crow, M.C. Anderson, C.R. Hain, D.M. Johnson, R. Mueller (2017). Intercomparison of Soil Moisture, Evaporative Stress, and Vegetation Indices for Estimating Corn and Soybean Yields Over the U.S., IEEE Journal of Selected Topics in Applied Earth Observations and Remote Sensing, 10(4): 1328-1343. doi:10.1109/JSTARS.2016.2639338 Article

Mladenova, I.E., Bolten, J.D., Crow, W.T., Sazib, N., Cosh, M.H., Tucker, C.J. and Reynolds, C., 2019. Evaluating the operational application of SMAP for global agricultural drought monitoring. IEEE Journal of Selected Topics in Applied Earth Observations and Remote Sensing, 12(9): 3387-3397. doi:10.1109/JSTARS.2019.2923555 Article

Mladenova, I.E., Bolten, J.D., Crow, W., Sazib, N. and Reynolds, C., 2020. Agricultural drought monitoring via the assimilation of SMAP soil moisture retrievals into a global soil water balance model. Front. Big Data, 3(10). doi:10.3389/fdata.2020.00010 Article

Müller, C., J. Elliott, J. Chryssanthacopoulos, A. Arneth, J. Balkovič, P. Ciais, D. Deryng, C. Folberth, M. Glotter, S. Hoek, T. Iizumi, R.C. Izaurralde, C. Jones, N. Khabarov, P. Lawrence, W. Liu, S. Olin, T.A.M. Pugh, D. Ray, A. Reddy, C. Rosenzweig, A.C. Ruane, G. Sakurai, E. Schmid, R. Skalsky, C.X. Song, X. Wang, A. de Wit, and H. Yang, 2017: Global gridded crop model evaluation: Benchmarking, skills, deficiencies and implications. Geosci. Model Dev., 10, 1403-1422, doi:10.5194/gmd-10-1403-2017.

O'Neill, P. E., S. Chan, E. G. Njoku, T. Jackson, and R. Bindlish (2016). SMAP L3 Radiometer Global Daily 36 km EASE-Grid Soil Moisture, Version 4. Boulder, Colorado USA. NASA National Snow and Ice Data Center Distributed Active Archive Center. doi:10.5067/ZX7YX2Y2LHEB

Rosenzweig, C., J.W. Jones, J.L. Hatfield, J.M. Antle, A.C. Ruane, and C.Z. Mutter, 2015: The Agricultural Model Intercomparison and Improvement Project: Phase I activities by a global community of science. In Handbook of Climate Change and Agroecosystems: The Agricultural Model Intercomparison and Improvement Project (AgMIP) Integrated Crop and Economic Assessments, Part 1. C. Rosenzweig and D. Hillel, Eds., ICP Series on Climate Change Impacts, Adaptation, and Mitigation Vol. 3. Imperial College Press, pp. 3-24, doi:10.1142/9781783265640_0001.

Rosenzweig, C., C.Z. Mutter, A.C. Ruane, E. Mencos Contreras, K.J. Boote, R.O. Valdivia, J. Houtkamp, D.S. MacCarthy, L. Claessens, R. Adhikari, W. Durand, S. Homann-Kee Tui, A. Ahmad, N. Subash, G. Vellingiri, and S. Nedumaran, 2021: Chapter 5: AgMIP regional integrated assessments: High-level findings, methods, tools, and studies (2012-2017). In Handbook of Climate Change and Agroecosystems: Climate Change and Farming System Planning in Africa and South Asia: AgMIP Stakeholder-driven Research, Part 1. C. Rosenzweig, C.Z.

Mutter, and E. Mencos Contreras, Eds., Series on Climate Change Impacts, Adaptation, and Mitigation Vol. 5. World Scientific, pp. 123-142, doi:10.1142/9781786348791_0005.

Sazib, N., Mladenova, I., & Bolten, J. (2020). Assessing the Impact of ENSO on Agriculture over Africa using Earth Observation Data. Frontiers in Sustainable Food Systems, 4, 188. doi:10.3389/fsufs.2020.509914 Article Google Scholar

Sazib, N., Mladenova, I. and Bolten, J., 2018. Leveraging the google earth engine for drought assessment using global soil moisture data. Remote sensing, 10(8): 1265. doi:10.3390/rs10081265 Article